Supplementary Figures and Legends

Supplementary Figure 1

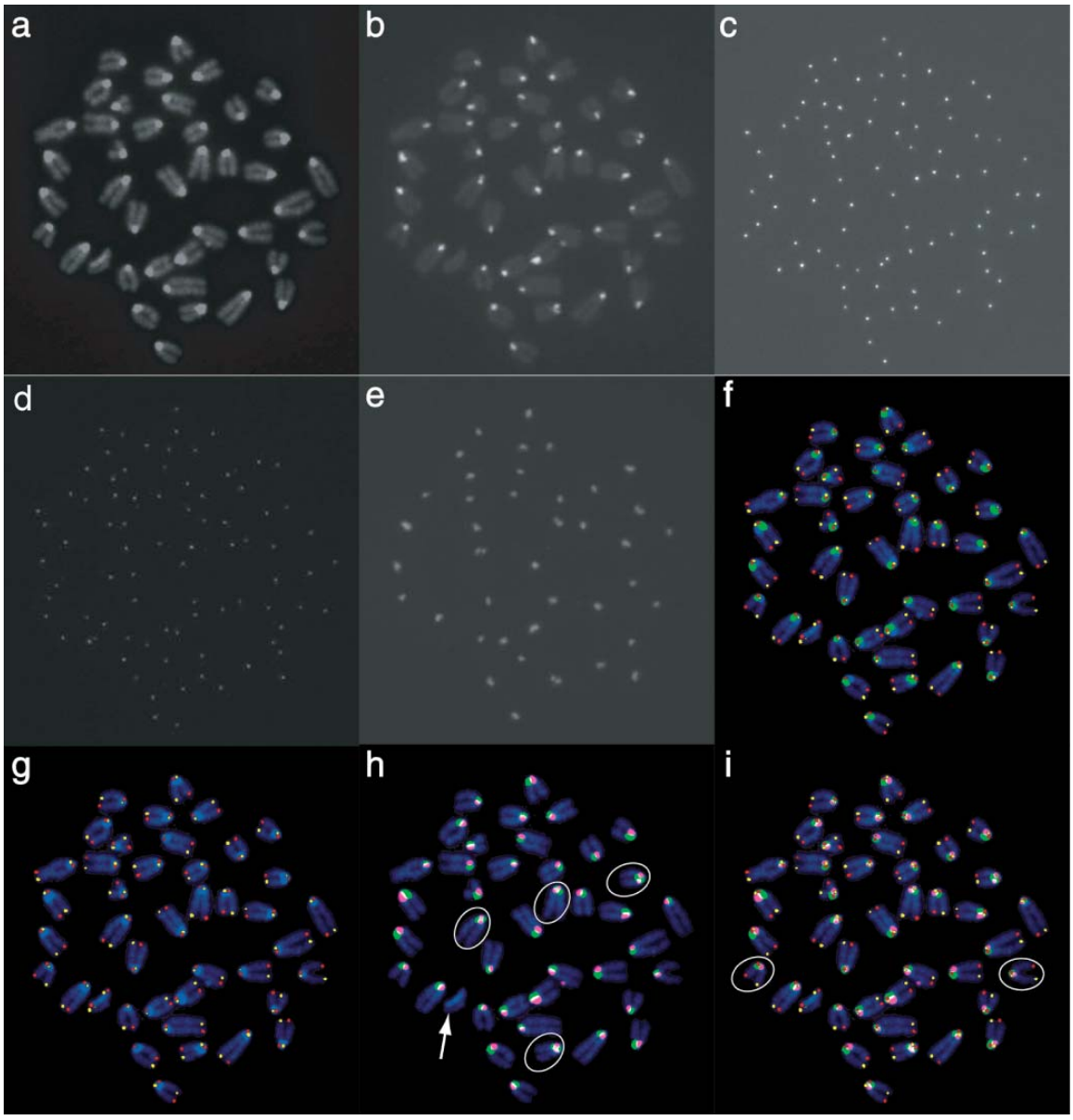

Supplementary Figure 1.

Orientation of major satellite and telomere repeats on mouse metaphase chromosomes using four-color CO-FISH. **a**, Raw image data of DAPI-stained *M. musculus* chromosomes in a clonal derivative of C2 (gift from Dr. A. Nagy, Toronto), a murine embryonic stem cell line derived from a C57BL/6NTac pre-implantation embryo.

Although this particular metaphase has 41 chromosomes (trisomy of chromosome 11) it illustrates the conserved orientation of major satellite repeats relative to telomere repeats. **b**, Raw image data of fluorescence obtained with fluorescein-labeled GACGTGGAATATGGCAAG PNA specific for the T-rich "Crick" strand of mouse major satellite DNA. **c,** Raw image data of the Cy5 fluorescence obtained with Cy5-labeled $(CCCTAA)_3$ PNA specific for G-rich telomeric DNA. **d,** Raw image data of the Cy3 fluorescence obtained with Cy3-labeled $(TTAGGG)_3$ PNA specific for C-rich telomeric DNA. **e**, Raw image data of the Texas Red (TxR) fluorescence showing Texas Red-labeled CTTCAGTGTGCATTTCTC PNA specific for the A-rich "Watson" strand of mouse major satellite DNA. **f**, Projection of signals obtained with probes specific for G-rich (shown in red), C-rich telomeric DNA (shown in yellow) and the A-rich strand of mouse major satellite DNA (shown in green). **g**, Projection of signals obtained with probes for G-rich and C-rich telomeric DNA shown in red and yellow, respectively). **h**, Projection of fluorescein-labeled PNA specific for the T-rich strand of mouse major satellite DNA (shown in purple) and TexasRed-labeled PNA specific for the A-rich strand of mouse major satellite DNA (shown in green). Note that 4 chromosomes (both homologs of chromosome 4 and 18, ellipses) have significant amounts of T-rich DNA on the "Watson" strand. **i**, Four-color image (Figure 1b in the original paper). Two chromosomes underwent a sister chromatid exchange event (red or yellow telomere probes hybridizing to the same sister chromatid: ellipses).

Supplementary Figure 2

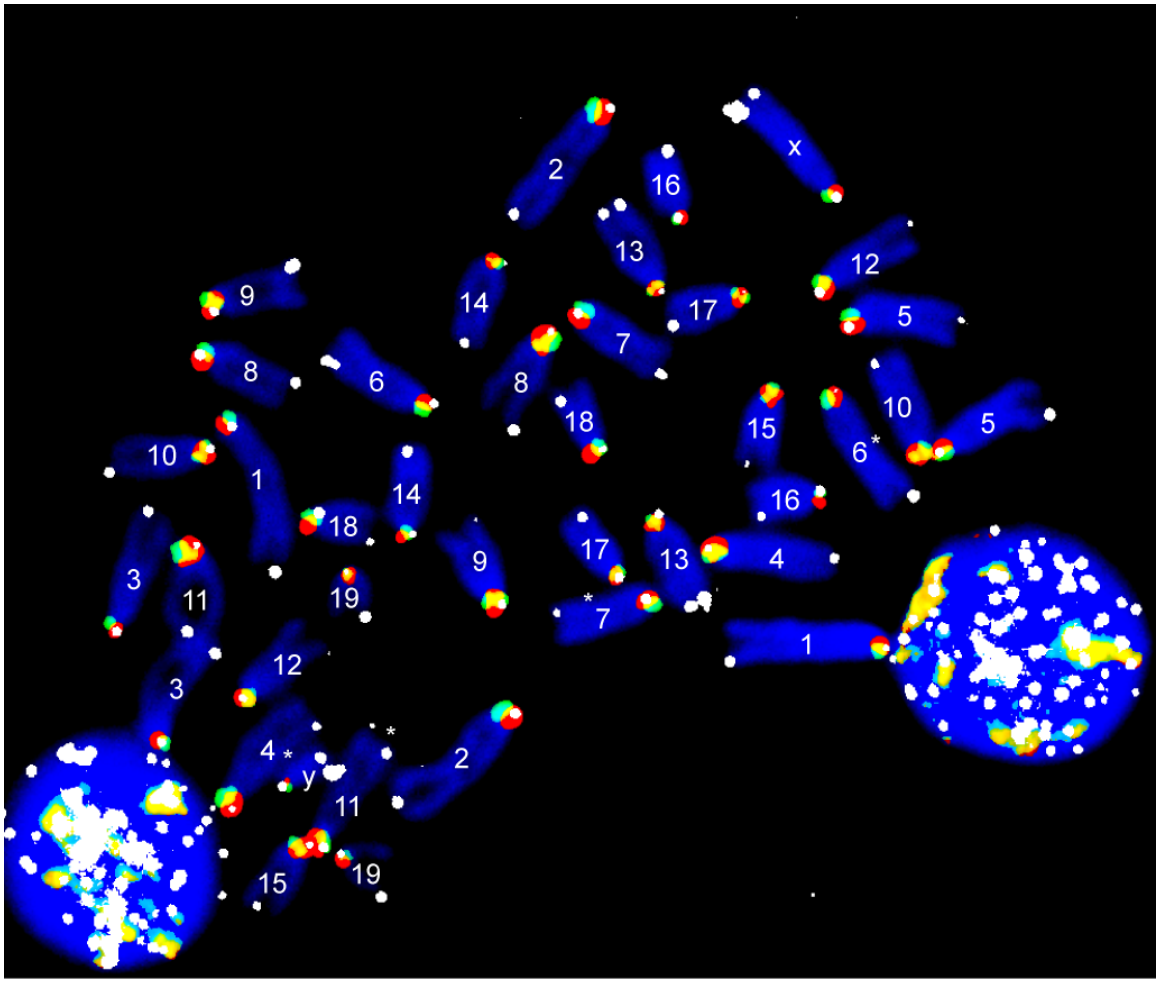

Supplementary Figure 2.

Conserved orientation of repetitive DNA in chromosomes from *M. spretus*. Pseudo-color image of metaphase chromosomes following four-color CO-FISH analysis with PNA probes specific for T-rich minor satellite DNA (fluorescein-labeled CGG CAT TGT AGA ACA GTG, shown in green), A-rich minor satellite DNA (Cy3-labeled CGG TTT CCA ACG AAT GTG shown in red) and G-rich telomeric DNA (Cy5-labeled $(CCCTAA)_3$, shown in white). Following CO-FISH, specific chromosomes were identified using M-FISH[36]. Fluorescence derived from the PNA probes was enhanced and given a pseudo-color using Adobe Photoshop for the purpose of illustration. Overlapping

red and green fluorescence (shown in yellow) only indicates bidirectional orientation of repetitive DNA if signals cross to both sister chromatids. Note that in all chromosomes except in chromosomes 16, 18 and 19 the Watson DNA template strand (containing A-rich minor satellite DNA shown as red dots) overlaps with the 3' telomere on the short arm characterized by a white dot. Minor satellite repeats are unidirectional on the larger chromosomes 1-8 as well as on chromosomes 11, 12, 14, X and Y. Smaller amounts of bidirectional minor satellite repeats are observed on chromosomes 9, 10, 13, 15 and 17. On these chromosomes the strand with T-rich minor satellites appears to be adjacent to the 5'telomere. Thus in 17 of 20 *M.spretus* chromosomes DNA template strands show a similar organization as in *M.musculus* with the 5' end adjacent to T-rich satellite DNA. Note that telomere repeats are unexpectedly bidirectional on chromosomes 13, X and Y. In some cases the orientation of repetitive DNA could not be assigned from this single metaphase spread because sister chromatids were overlapping or could not be clearly distinguished, PNA fluorescence signals from telomeric and minor satellite repeats was overlapping or template strands showed sister chromatid exchange events (asterisks). However, the pattern described here was confirmed by combined CO-FISH/M-FISH analysis of additional metaphases. For preparation of metaphase cells, fibroblast derived from lung tissue of adult (6 weeks old) *M. spretus* mice (SPRET/EiJ; Stock Number 001146, Jackson Laboratory, Bar Harbor, Maine) were grown in the presence of 40 μM BrdU for 16 hours prior to harvesting. The last 2 hours of culture were in the presence of 0.1 μg/ml of colcemid to block cells in metaphase. CO-FISH was performed as described in the Methods section.

Supplementary Figure 3

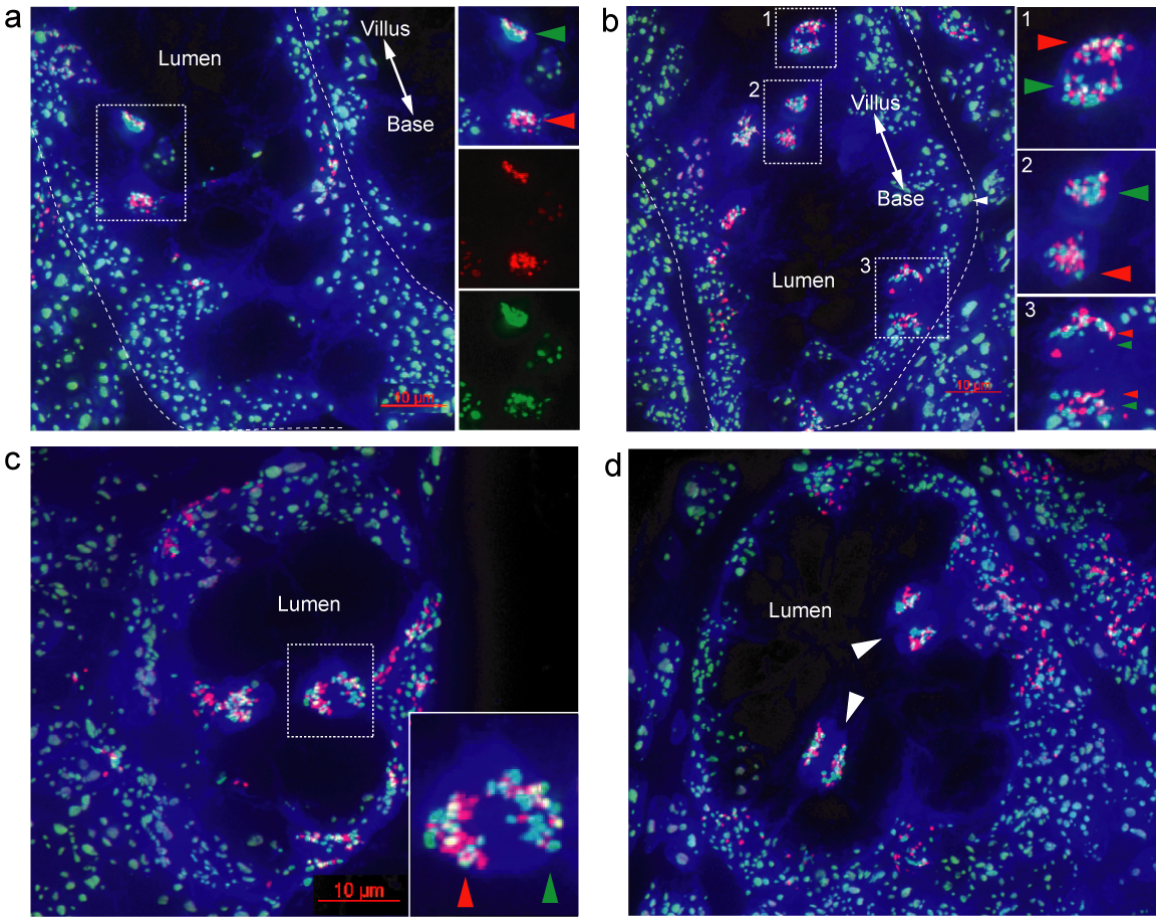

Supplementary Figure 3.

Variable spatial orientation and location of cells showing apparent asymmetric distribution of defined DNA template strands. **a**, A pair of cells showing asymmetric template strand segregation with the axis of division parallel to the axis of the intestinal crypt. In this case, the daughter cell oriented towards the base of the crypt (outlined with a white dashed line) contained the majority of Watson strands, whereas the daughter oriented towards the villus contained the majority of Crick strands (right panels and red and green arrows). **b**, In some cases, it was not possible to correlate asymmetry of strand distribution with crypt position. Two pairs of cells in the same crypt with asymmetric

fluorescence distribution (boxed 1 and 2, and right panels), displayed opposite orientation of the Watson-fluorescence-enriched daughter cells (red arrows, right panels 1 and 2) relative to the base of the crypt. A third cell pair (boxed 3 and right panel) showed a more symmetric distribution of Watson and Crick fluorescence. This panel appears in the manuscript as Figure 2c. **c**, In some images, cells showing clear CO-FISH signals appeared to be dividing perpendicular to the crypt axis (boxed), with one cell projecting into the lumen, and one cell remaining close to the crypt wall. **d**, However, this orientation was not always observed, since some of these cell pairs appeared equidistant from the crypt wall, with neither daughter cell projecting into the lumen (arrowheads).

Supplementary Figure 4

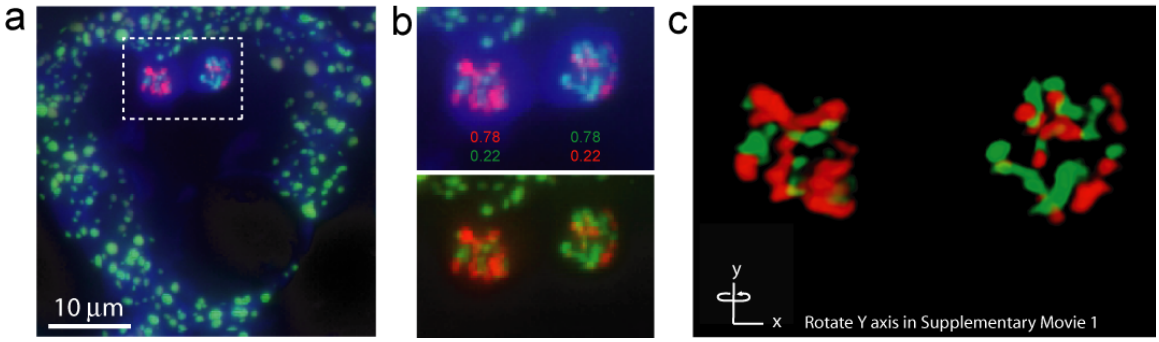

Supplementary Figure 4.

DNA template strand asymmetry in post-mitotic colon cells. **a**, Image stack projection of a cross section of a colon crypt that was subjected to CO-FISH. Note the pair of post-mitotic cells (boxed) with clear non-overlapping CO-FISH signal surrounded by non-dividing colon crypt cells not showing discrete red and green fluorescence. **b**, Magnification and measured relative fluorescence of boxed cells shown in **a**. The red and green fluorescence in each cell was quantified as described (see Supplementary Methods and Figure 3) and corresponds to the proportion of Watson and Crick template strands inherited by each daughter cell. **c**, 3-D rendering of the cell pair shown in **a** and **b** using Volocity (V4.1.0, www.improvision.com) software. Note the reciprocal asymmetry of red and green fluorescence. This rendering can be viewed from different angles in Supplementary Movie 1.

Supplementary Figure 5

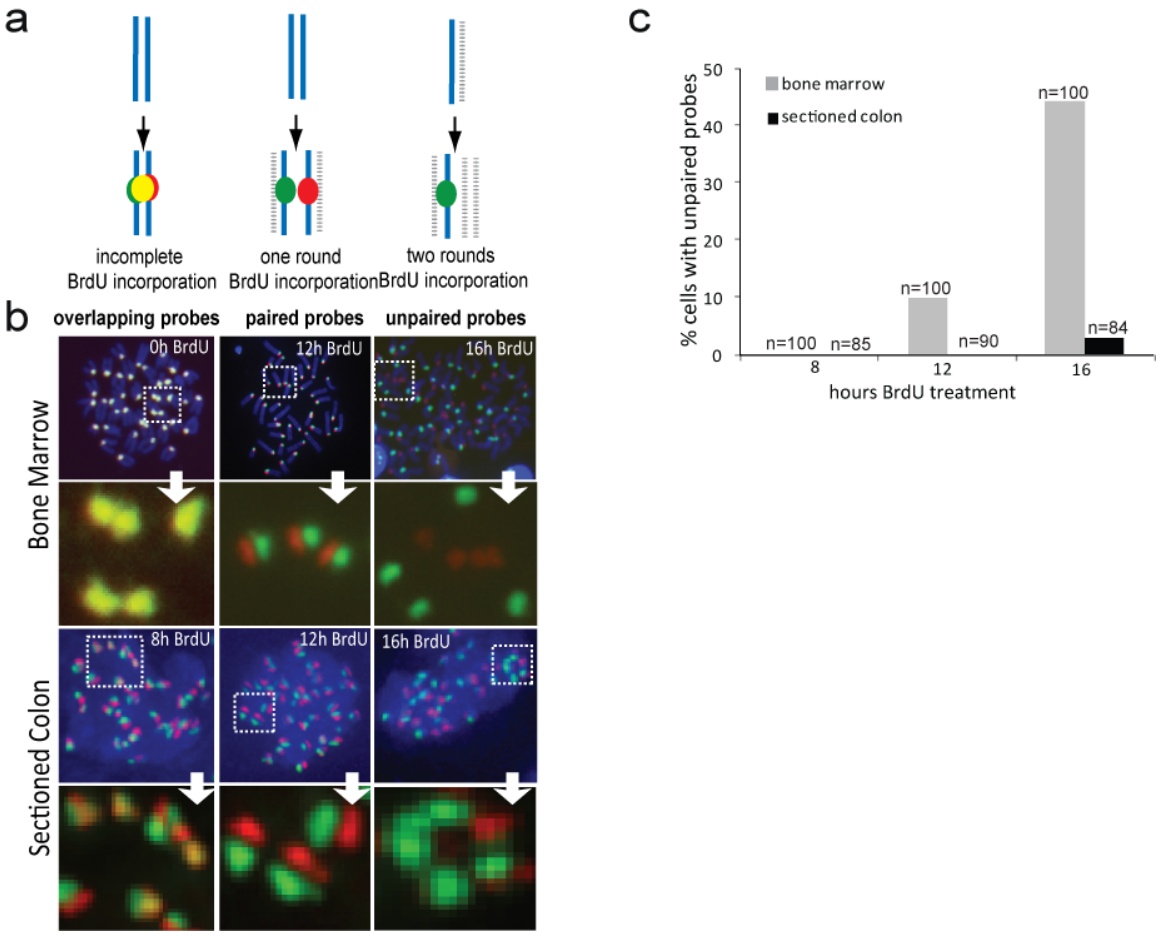

Supplementary Figure 5

Colon cells divide only once during 12 hour BrdU treatment. **a**, Assay for paired probe signals in metaphase-arrested cells from bone marrow and colon treated with 0, 8, 12 or 16 hourly injections of BrdU. **b**, Fluorescence signals from major satellite probes in metaphase-arrested mitotic cells from bone marrow and colon cells. Double stranded chromatids (incomplete or no DNA replication) show overlapping yellow probe fluorescence signals (left column) while two rounds of DNA replication result in unpaired, single probe signals (16 hours BrdU, right column). Only a single complete round of DNA replication results in single-stranded CO-FISH chromosomes, and paired

non-overlapping major satellite probe signals (12 hours BrdU, middle column). **c**, Assay for unpaired probe signals indicating two rounds of DNA synthesis during BrdU treatment. While bone marrow cells exhibit a faster mitotic cycle, sectioned colon cells divide only once during 12 hour BrdU treatment. Only 3% of colon cells treated for 16 hourly BrdU injections showed unpaired major satellite probes, indicating a low percentage of second round DNA synthesis, and a slower mitotic cycle than bone marrow cells.

Supplementary Figure 6

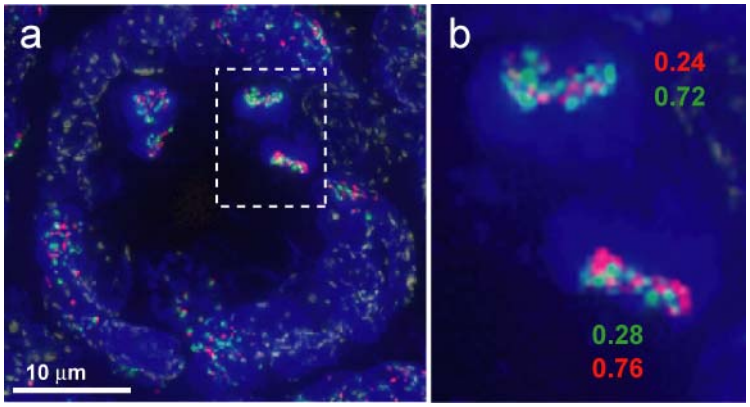

Supplementary Figure 6.

DNA template strand containing A- or T-rich minor satellite DNA do not appear randomly distributed in a subset of post-mitotic colon cells derived from *M. spretus*. **a**, Image stack projection of a colon tissue section from *M. spretus* following CO-FISH using PNA probes specific for minor satellite repeats (see Supplementary Figure 2 for details). A pair of post-mitotic cells (boxed area) shows clear CO-FISH signals. **b**, Quantification of fluorescence signals in *M. spretus* colon crypt cells shows asymmetric distribution of DNA template strands defined by strand-specific minor satellite repeats. Note the reciprocal relationship between red and green fluorescent signals.

Supplementary Figure 7

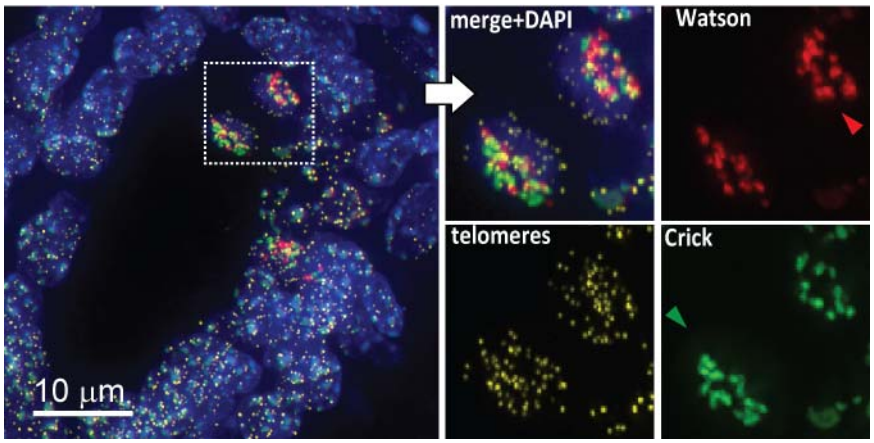

Supplementary Figure 7.

Preservation of nuclear architecture following CO-FISH in fixed colon tissue sections. 3-color CO-FISH using a A-rich and T-rich major satellite probes (red and green fluorescence) and a telomere probe (yellow fluorescence; see Supplementary Figure 1d) showing that position of major chromosomal features, telomeres and pericentric regions does not appear to be affected by BrdU treatment and the CO-FISH procedure (boxed areas and right panels)

Supplementary Figure 8

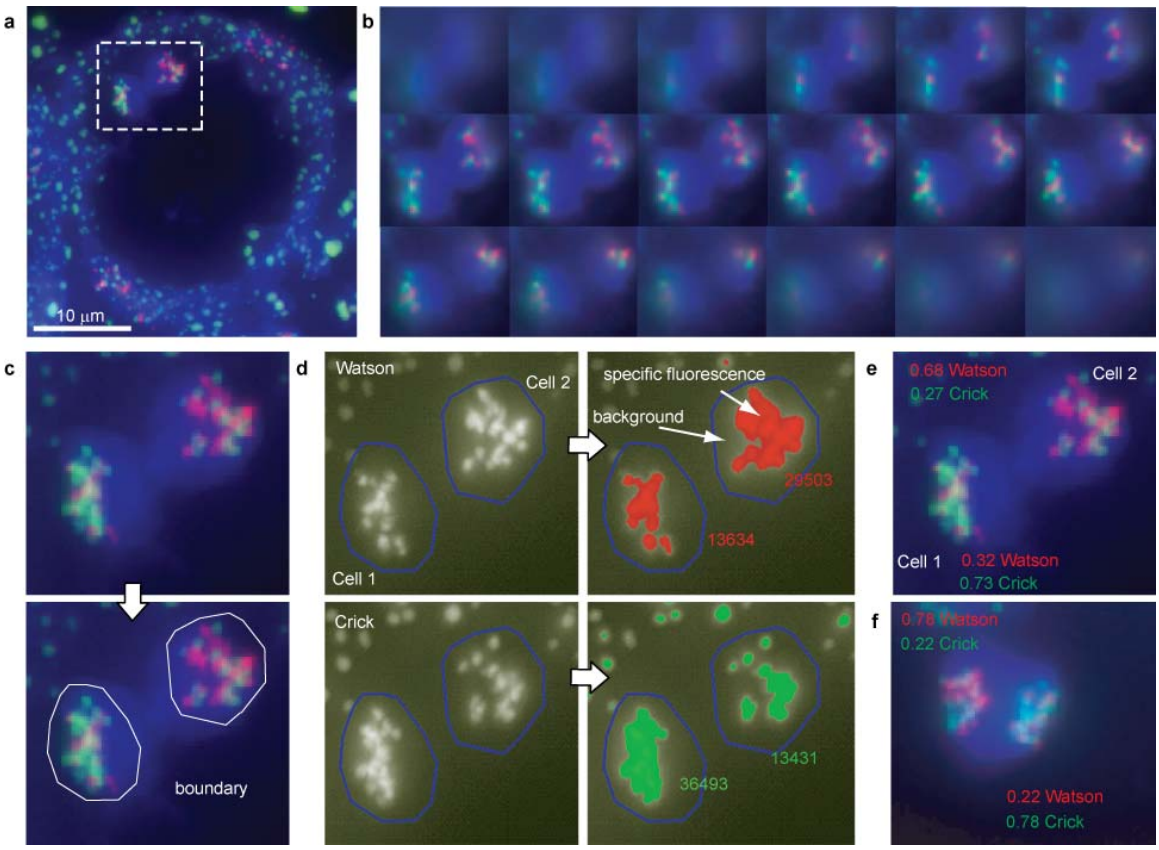

Measurements of CO-FISH fluorescence from image stacks **a**, Image projection of images acquired at 0.2 micron intervals. **b,** Focal plane mages of boxed area shown in (**a**) at 0.6 micron intervals **c**, Boundary drawn around nuclear area based on DAPI fluorescence. **d**, Specific fluorescence was measured following subtraction of background fluorescence within the defined nuclear boundaries. Calculated fluorescence values for each daughter nucleus (red and green numerical values) were converted to relative fluorescence (**e**) and normalized to 1 between both daughters. **f**, Example of reciprocal Watson and Crick fluorescence distributions in pairs of post-mitotic daughter cells.

Supplementary Figure 9

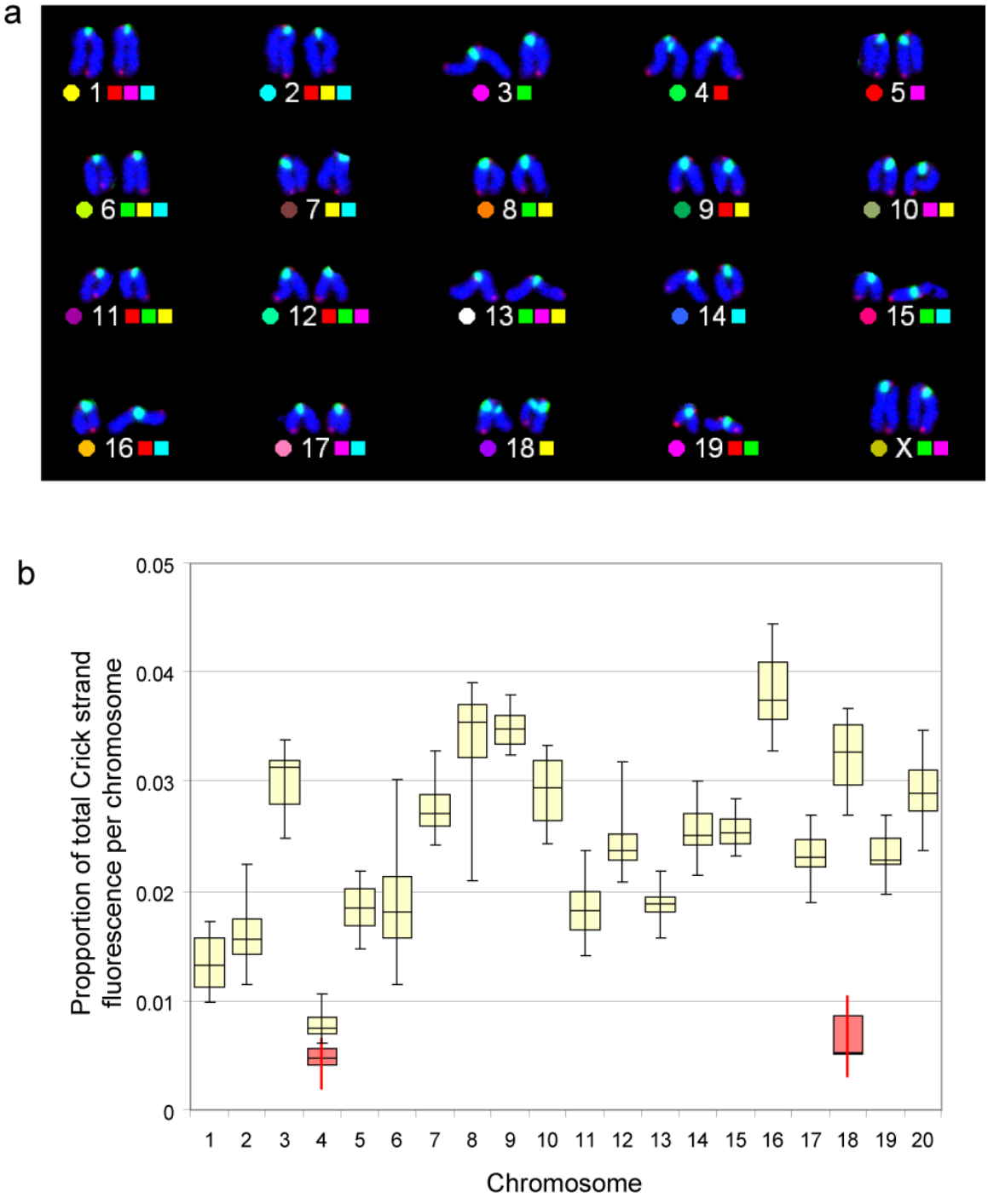

Supplementary Figure 9.

Distribution of T-rich major satellite DNA on specific chromosomes **a**, CO-FISH images of fluorescein-labeled PNA specific for T-rich major satellite DNA on the Crick DNA template strand were acquired, followed by karyotyping of the chromosomes using M-FISH[36]. The color scheme of the M-FISH probes is shown below the images of the major satellite CO-FISH fluorescence of each chromosome (shown in yellow) counterstained with DAPI (shown in blue). Note that homologous chromosomes show very similar fluorescence intensities and chromosomes 4 and 18, unlike all other chromosomes, show fluorescence signals on both sister chromatids. **b,** Chromosome-specific major satellite CO-FISH fluorescence intensity values derived from 6 female metaphase cells that were karyotyped by M-FISH. The measured intensity of each of the 20 murine chromosomes in these cells was normalized per metaphase to allow comparisons of major satellite fluorescence between chromosomes. A box plot (12 data points per chromosome) shows differences in major satellite fluorescence amongst chromosomes. Boxed areas represent 25-75% of values (median is bold horizontal line) and thin vertical lines represent the 5 and 95 percentile of data points.

Supplementary Figure 10

a

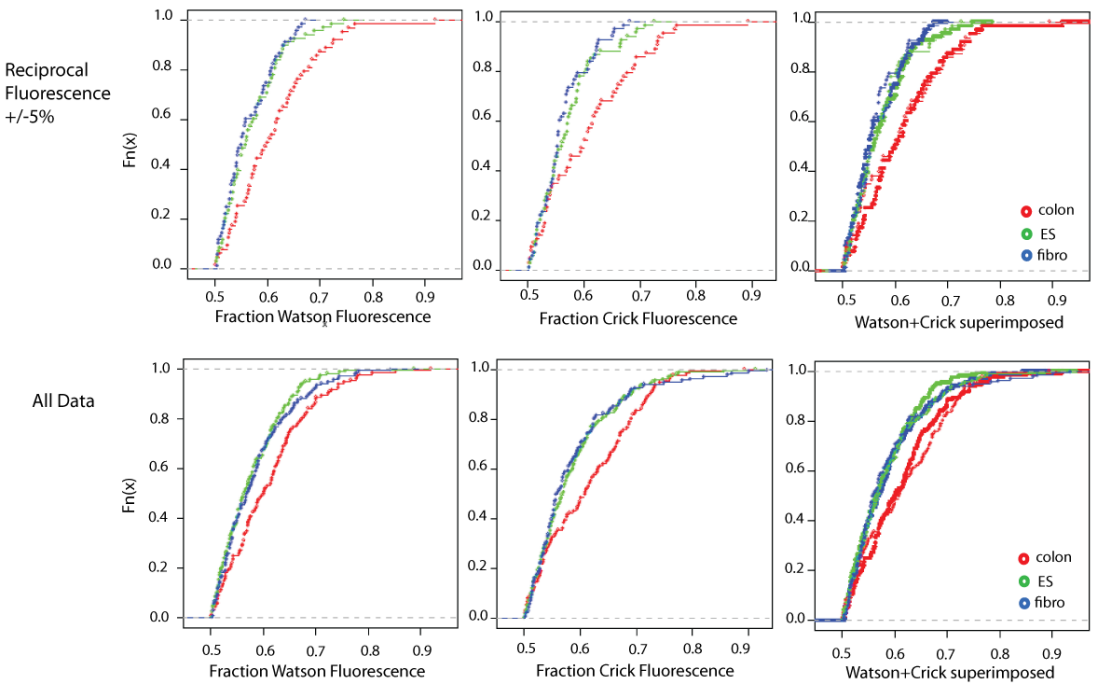

b

Associated p-values of Kolmogorov-Smirnov tests

Reciprocal Fluorescence +/-5%

Data set comparisons/N set 1	set 2	p-values Watson	Crick	Watson-Crick comparisons/N	p-values
Colon/63	ES/68	**0.0198**	**0.0018**	Colon/63	0.6943
Colon/63	Fibro/68	**0.0010**	**0.0009**	ES/68	0.9563
ES/68	Fibro/68	0.8676	0.3378	Fibro/68	0.5943

All Data

Data set comparisons/N set 1	set 2	p-values Watson	Crick	Watson-Crick comparisons/N	p-values
Colon/132	ES/161	**0.0016**	**0.0015**	Colon/132	0.3615
Colon/132	Fibro/136	**0.0107**	**0.0009**	ES/161	0.8466
ES/161	Fibro/136	0.8853	0.8710	Fibro/136	0.8558

Supplementary Figure 10

Kolmogorov-Smirnov analysis of cumulative fluorescence distributions derived from Watson and Crick strands in sectioned colon (red), cultured embryonic stem cells (green), and cultured lung fibroblasts (blue). Fluorescence distributions in colon cell pairs are significantly different than for cultured mouse embryonic stem cells (ES) and lung fibroblasts (fibro). **a**, Cumulative distribution curves show that colon cell Watson and Crick fluorescence distribution (red) differs from cultured ES (green) and fibroblast (blue) cell distributions. The difference is maintained when examining the selected reciprocal ratio data set (top row, reciprocal ratios +/- 5%, corresponds to filled squares in manuscript Figure 3h), and the entire data set (bottom row, correspond to open circles in manuscript Figure 3h). Furthermore, superimposing Watson and Crick distribution curves shows that Watson and Crick distributions for each data set are nearly identical (right panels). **b**, Associated p-values of pair-wise K-S tests of cumulative distribution confirms that both Watson and Crick fluorescence distributions in colon cells are significantly different compared to ES and fibroblast cell distributions (bold, left panel). By comparison, ES and fibroblast distributions do not significantly differ from each other. Furthermore, K-S comparison of superimposed Watson and Crick distributions yields no significant differences, for any cell type tested (right panels).

Supplementary Figure 11

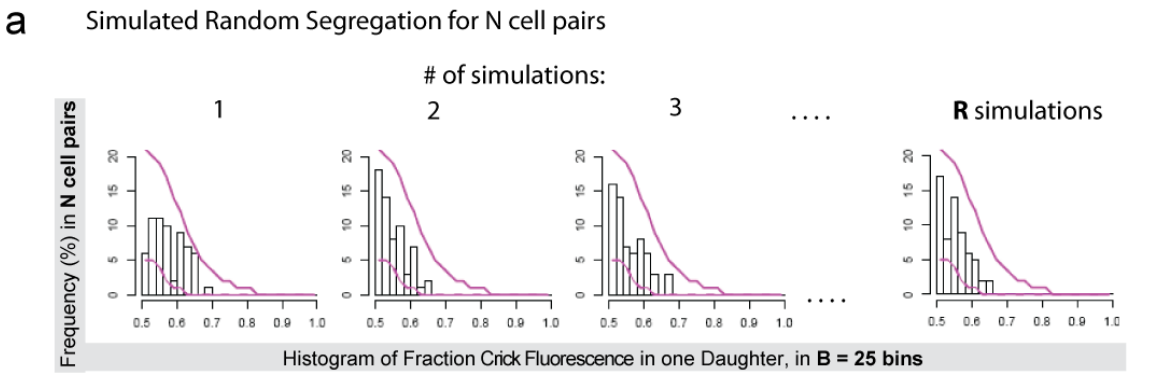

Sorted bin heights for each bin define curve-wise envelopes for random segregation, 99% and 95% confidence intervals (CI) were calculated from these curve-wise envelopes.

Supplementary Figure 11

Generation of curve-wise envelopes for simulated random segregation. Algorithm was adapted from Davison and Hinkley[36]. **a**. Random segregation was simulated R times for N observed cell pairs, as described in Supplementary Notes. Fraction of Crick fluorescence in one daughter cell was binned into 25 bins (B; X-axis) as described. **b**. A simulation matrix (M) was created using R simulations (rows) and B bins (columns). Each cell in the matrix represents one Crick fluorescence histogram bar for one bin, in one simulation. The histogram bar height was recorded. **c**. The histogram heights were then ranked from maximum to minimum for each bin. The u^{th} and ℓ^{th} rows of the sorted matrix represent the curve-wise envelopes for expected Crick fluorescence in simulated random segregation. Rows u and ℓ were chosen so as to yield 95% and 99% confidence intervals (curve-wise envelopes illustrated with purple curves in **a** were constructed so that 95% or 99% of all simulated histograms lie entirely within the curve-wise envelope).

Supplementary Notes

Quantitative image analysis.

Multi-wavelength single-plane CO-FISH images from slides with cultured cells and average projections of image stacks from colon tissue sections were used for quantitative analysis. The integrated fluorescence intensity from fluorescently-labeled PNA probes hybridized to major satellite repeats on either Watson or Crick DNA template strands (See Figure 1) was measured from these images. For this purpose, metaphase chromosomes or nuclei of daughter cell pairs were identified using Isis (V5, MetaSystems Group Inc., Watertown, MA) or SoftWoRx Explorer (V1.2, Applied Precision LLC, Issaquah, WA) software.

To measure the relative amount of Watson and Crick template strands in each cell pair we developed dedicated software (Supplementary Figure 8). First, a border around the nucleus of each daughter cell was drawn manually, using DAPI fluorescence as a visual aid (Supplementary Figure 8c). Next, the area of Watson probe fluorescence was determined by using the intensity threshold level (pseudo-colored as red) that segmented the area encompassing pixels of interest above the threshold level. The background level was determined as the median intensity level of all pixels below the selected threshold level within the drawn nuclear boundary. The specific fluorescence value for the Watson strand probe was calculated in drawn areas by summation of all pixel values above the threshold after subtraction of the median background pixel value for each pixel. This approach was repeated for the Crick probe (pseudo-colored as green). The raw data encompassing all fluorescence measurements for all cells are presented in an Excel spreadsheet as Supplementary Data Table.

To estimate the variation of probe hybridization to Watson and Crick template strands of sister chromatids, the TFL-Telo[37] software (available from www.flintbox.com) was used to segment single-stranded metaphase chromosomes (Figure 1a) and measure the individual fluorescence signals (spots) for each chromatid. This analysis (shown in Figure 1b) revealed an excellent correlation (R=0.93) between signals from homologous chromosomes using probes specific for A- and T-rich major satellite DNA. To estimate the variation in the amount of major satellite probe hybridizing to specific chromosomes, we combined M-FISH[38] karyotyping with CO-FISH using fluorescein-labeled GACGTGGAATATGGCAAG PNA probe specific for the T-rich "Crick" strand of mouse major satellite DNA repeats (See Supplementary Figure 9). This analysis was repeated for karyotyped chromosomes derived from 6 metaphase cells of C57BL/6J bone marrow cells. The relative major satellite fluorescence of each chromosome was used to model expected fluorescence values in simulated random segregation models.

Statistical analysis and considerations

It is impractical and difficult to compare the raw fluorescence intensity estimates of probes hybridized to the Watson strand with those hybridized to the Crick strand, and between different daughter cell pairs, due to differences in the exposure times used to acquire individual images and differences in the number of images per image stack. Hence, we normalized the fluorescence measurements based on the assumption that for each chromosome, the Watson template will be segregated to one daughter while the Crick template will be segregated to the other daughter. Therefore, it is expected that the total amount of Watson plus Crick probes in each daughter cell is equivalent and follows

a reciprocal relationship because a fixed number of templates from a single mother were distributed to the two daughter cells. The total fluorescence obtained with each probe in both daughter cells is normalized to 1.

It is important to note that random segregation is expected to include some marked asymmetric events, much like randomly flipping a coin many times will result in a heads:tails ratio that centers around 50:50 but will deviate from a strictly equal distribution. Therefore, we attempted to test significance of the measured asymmetry in colon cells by comparing the observed distribution of fluorescence from our measurements to the expected distributions obtained from simulated random segregation. We modeled our statistical approach on the assumption that the distribution of Watson and Crick strands to daughter cells A and B can be modeled as a weighted binomial process with N=40 as the total number of Watson template strands and p_A as the proportion of Watson strands directed to Daughter A. On average, about 20 of the Watson strands will go to daughter cell A, though this number will vary, with frequency illustrated by the binomial distribution. However, daughter cells A and B are mirror images with respect to strand distribution, and are therefore not independent. In addition, the nature of sectioned colon tissue and cultured cells is such that we cannot use positional information to distinguish between daughters. This means it is not possible to assign either daughter cell as being "A" or "B" within a data set. If there is no way to differentiate between daughter cells A and B, then we cannot identify and measure p_A directly. In this case we can only observe that a proportion of the total (X) Watson strands ended up in one daughter cell while the rest (40-X) ended up in the other daughter cell, which makes the distribution a "folded" binomial. For example, a 30% Watson

proportion in daughter A is mirrored as a 70% proportion in daughter B, making the binomial folded around the 50% probability. Hence, since the fluorescence intensity measured in only one of the daughter cells matters for the statistical analysis, we arbitrarily chose one daughter cell, with the greater proportion of Watson or Crick probe fluorescence: X_{max}=max(X, 40-X), from each pair to compare observed fluorescence values to a simulated random distribution.

In order to test whether the observed data were consistent with a random model (a binomial model with a proportion p=0.5 of Watson strands directed to one daughter cell), a combination of bootstrapping and Monte Carlo simulation[36] was performed to derive 95% and 99% confidence bounds for fluorescence distributions expected by chance. To determine fluorescence values to use in simulated segregations, the major satellite fluorescence of Crick template strands was measured in each of the 20 murine chromosomes from six CO-FISH metaphase preparations (Supplementary Figure 9). Crick fluorescence values for all chromosomes was randomly chosen from these six metaphase cells and randomly assigned to one of the two daughter cells to simulate random sister chromatid segregation. This approach takes into account the variable fluorescence at specific chromosomes, and by randomly choosing between six measured metaphase values, the variability of measurement between different cells is taken into account. After all chromosomes were "segregated" for one cell, the total simulated "inherited" Watson and Crick fluorescence was tallied for each daughter (W1 and W2, G1 and G2). The random segregation was repeated for N observed cell pairs for each cell type, to complete one simulation data set, and a corresponding folded histogram (again, by taking the greater of the two simulated Crick proportions = max(G1, G2)) was plotted.

This process of simulating the data set was repeated 100,000 times to generate curve-wise envelopes containing 95% and 99% of the simulated histograms shown in Figure 3c. (A detailed description of the algorithm for construction of these curve-wise envelopes is provided in the last section of Supplementary Materials, and Supplementary Figure 11). If any portion of the observed histogram of values lies outside of the 95% envelope, this provides evidence against the null hypothesis of random distribution of Watson strands at the 5% level (i.e., simulation $p < 0.05$). If a portion of the observed histogram lies outside the 99% envelope, this provides evidence against the null hypothesis at the 1% level, that is, the simulation p-value is less than 0.01. Barring measurement error and other external noise, the Watson and Crick data should yield identical results. The observed histogram of values for the colon cells exceeded the 95% and 99% simulation histogram envelope for both Watson and Crick strand data, yielding a simulation p-value < 0.01. This suggests our observed data are inconsistent with an underlying 50/50 binomial model. There is an excess of events in the right tail of the histogram that is consistent with the hypothesis that Watson or Crick strands are directed to a daughter cell (under a mixed model) such that a fraction of the cells have a proportion greater than 0.5 (multiple peaks in our observed histogram). The conclusion that the fluorescence distribution of Watson and Crick strands in colon cells is significantly different than in cultured embryonic stem cells and fibroblasts is also supported by an independent test using the two-sample Kolmogorov-Smirnov (K-S) statistic (Supplementary Figure 10).

We deemed our statistical analysis combining bootstrapping and Monte Carlo simulations as the most appropriate method to analyze our observed data[39]. It's important to note that the generation of the curve-wise envelopes in the simulated segregations

assumes that each chromatid segregates independently of other chromatids. However, it's possible that different cell types asymmetrically segregate groups of chromatids, but in lieu of chromatid-specific probes and identification of different cell types in the colon, we are unable to incorporate this possibility into our simulations.

Algorithm for construction of curve-wise envelopes

To generate curve-wise envelopes, we adapted the methodology outlined in Davison and Hinkley pp150-154 (herein referred to as D&H)[36]. Briefly, let R be the number of simulations (corresponds to the R simulations in D&H. Let B be the number of histogram bins (= 25; corresponds to the N order statistics in D&H) Let N be the number of independent data realizations (corresponds to number of cell pairs; no direct analogue in D&H). Each of the R simulation runs yields a histogram of the N cell pairs in B = 25 bins (Supplementary Figure 11a). We then record the bin heights for i^{th} simulation run in row i of a matrix M with dimension R x B (R rows and B columns, Supplementary Figure 11b).

Let Mij equal the height of the j^{th} histogram bin in the i^{th} simulation run, i = 1, 2, ...,R and j = 1, 2, ...,B. We denote the i^{th} row of M as M[i, .] and the j^{th} column of M as M[., j].

After recording the individual histogram bin heights for all R simulations, we sort each column of M in decreasing order (we denote the column-sorted matrix as Ms, Supplementary Figure 10c). Thus Ms[1, .] contains all the maximum bin bar heights and Ms[R, .] contains all the minimum bin bar heights. All R simulation histograms are

contained within the envelope with upper bound Ms[1, .] and lower bound Ms[R, .] (Supplementary Figure 11c).

Let alpha in (0, 1) be the desired type I error rate for the null hypothesis test, and (1 - alpha) be the corresponding confidence level. A 1-alpha confidence envelope is constructed by finding the largest (u^{th} for "upper") and smallest (l^{th} for "lower") rows of Ms such that alpha/2 of the simulated histograms show at least one histogram bar height Mij larger than Ms[u, j], and alpha/2 of the simulated histograms show at least one histogram bar height Mij smaller than Ms[l, j].

Simulation code implemented in the open source R language for generation of simulated segregation is available upon request.

References

[36] Davison, A.C. & Hinkley, D.V., *Bootstrap methods and their Application*. (Cambridge University Press, New York, 1997).

[37] Poon, S.S. & Lansdorp, P.M., Measurements of telomere length on individual chromosomes by image cytometry. *Methods Cell Biol* 64, 69-96 (2001).

[38] Geigl, J.B., Uhrig, S., & Speicher, M.R., Multiplex-fluorescence in situ hybridization for chromosome karyotyping. *Nat Protoc* 1 (3), 1172-1184 (2006).

[39] Dufour, J.M., Farhat, A, Exact nonparametric two-sample homogeneity tests for possibly discrete distributions. . *Cahiers de recherche 2001-23, Centre interuniversitaire de recherche en économie quantitative, CIREQ.* (2001).

Supplementary Video Legends

Supplementary Video 1

Distribution of defined DNA template strands in paired daughter cells in mouse colon analyzed by CO-FISH. See also Supplementary Figure 4. This movie shows an example of skewed, reciprocal distribution of green and red fluorescence obtained with major satellite probes specific for major satellite probes present on Watson (red) and Crick (green) template strands. The image stack of a mouse colon cross section was deconvolved using SoftWoRx (Applied Precision) software and rendered as a 3D image using Volocity (V4.1.0, www.improvision.com) software to enable inspection of red and green fluorescence from multiple angles.

Supplementary Video 2

Distribution of defined DNA template strands in paired metaphase chromosomes in the mouse colon analyzed by CO-FISH. See also figure 2f. This movie shows an example of apparent polarity of metaphase chromatids, with green and red fluorescence of the major satellite probes aligning in a polar fashion. The image stack of a mouse colon cross section was deconvolved using SoftWoRx (Applied Precision) software and rendered as a 3D image using Volocity (V4.1.0, www.improvision.com) software to enable inspection of red and green fluorescence from multiple angles.

Supplementary Video 3

Mirror asymmetry of defined DNA template strands in a pair of post-mitotic mouse colon cells. See also Figure 2g (top panels). This movie shows clustering of green and red CO-

FISH fluorescence obtained with PNA probes specific for major satellite sequences present on Watson (red) and Crick (green) template strands. Note that while the amount of red and green fluorescence in the two cells seems similar, the localization of red and green fluorescence within the nucleus appears to be clustered and shows mirror asymmetry over the two daughter cells. The image stack of a mouse colon cross section was deconvolved using SoftWoRx (Applied Precision) software and rendered as a 3D image using Volocity (V4.1.0, www.improvision.com) software to enable inspection of red and green fluorescence from multiple angles.

Supplementary Video 4

Mirror asymmetry of defined DNA template strands in a pair of post-mitotic mouse colon cells. See also Figure 2g (bottom panels). This movie shows clustering of green and red CO-FISH fluorescence obtained with PNA probes specific for major satellite sequences present on Watson (red) and Crick (green) template strands. Note that while the amount of red and green fluorescence in the two cells seems similar, the localization of red and green fluorescence within the nucleus appears to be clustered and shows mirror asymmetry over the two daughter cells. The image stack of a mouse colon cross section was deconvolved using SoftWoRx (Applied Precision) software and rendered as a 3D image using Volocity (V4.1.0, www.improvision.com) software to enable inspection of red and green fluorescence from multiple angles.

Supplementary Data Legend

Excel spreadsheet of relative fluorescence measurements extracted from two-color digital CO-FISH images of cell pairs present in colon tissue sections, colon suspension cells, fibroblast and ES cells (see also Methods, Supplementary Methods and Figure 3). Fluorescence values obtained with probes specific for major satellite sequences in the Crick DNA template strand (green fluorescence, G) and Watson DNA template strand (red fluorescence, R) were measured from projections of multi-focal-plane images in pairs of adjacent cells (1,2) which appeared intact and non-overlapping upon visual inspection prior to data acquisition. The fluorescence values (R1, R2, G1, G2) are the integrated fluorescence intensity of individual cells obtained by the summing the intensity levels of all pixels above a selected threshold within a selected cell boundary (area1, area2, in pixels). Pixels above the selected threshold fluorescence within selected cell boundaries are indicated as area_R1, area_G1, *et cetera*. Within this area, background fluorescence is subtracted (Backgnd_R1, Backgnd_R2, *et cetera*) for each pixel. Background fluorescence was calculated for each cell by selecting the median pixel fluorescence intensity that is within the selected cell boundary (area1, area 2 in pixels) but below the selected threshold. To normalize the integrated fluorescence measurements, we assumed Watson and Crick template strands from the parent cell are distributed between the two daughter cells. The ratio of the total integrated fluorescence in each daughter cell then becomes the relative fluorescence value (R1_ratio = R1/[R1+R2). The strength of the reciprocal relationship between the Watson and Crick strand distribution between daughter cells (i.e. R1_ratio ≈ G2_ratio and R2_ratio ≈

G1_ratio) is shown by max_RG_total is calculated as the larger of (R1_ratio+G1_ratio) or (R2_ratio+G2_ratio). Image files are available upon request.

Supplementary Data Image Gallery Legend

This image gallery shows cell pairs and surrounding tissue from statistically significant asymmetric segregation events. Quantified Watson (red) and Crick (green) template strand fluorescence ratios are indicated. Where possible, crypt positions are illustrated.